

Charge Transport in Molecular Wire-Effect of Orientation

Amardeep, Vijay kr. Lamba



Abstract: In this work, the novel method is introduced to simulate the electrical transport of nanoscale structures. We think of an open-ended quantum system (structural electrons) accelerated by the external energy from the electron and the energy that is dispersed by a small amount of heat using warm baths (electrons) operating in the electronics. We use periodic boundary conditions and use The Density Functional Theory to also eliminate the problem of multiple particles acting on a single-field problem. By explicitly treating corruption in the electrodes, the behaviour of the powerful is the result of our approach, with variations in propagation methods based on the Landauer process.

Keywords: NEGF, Two Probe System, Molecular Electronics, Scattering, Tunnelling.

I. INTRODUCTION

The continued decline in electronic widgets has raised modern challenges in the semiconductor construction. For every one generation of a new device, which focuses on a single nanometre scale, quantum effects are emerging and things that worked well for generations of the previous device, are not doing well. Thus, not only the latest materials demand to be introduced to vital operating principles for devices and geometries further demand to be updated. [1-6] Here, we centre on the charge transfer on the cell wall between two electrons that are in line with the goal of building devices out of possession of molecules and that are specific to electronic transfer conditions in numerous chemical & biological systems. [7 -10] We have used molecular wires made of "Benzene" repeating units to understand the cost distribution mechanism as it allows one to study the relative and nonlinear transport, spinning effect, temperature dependence, atom configuration, molecule-electrode interactions and the outcome of spinning of the chemical layer. Experimental tasks performed by various categories provided additional information on the effects of the inputs and the charging processes on charging. [11-12] Calculations performed on an individual workstation.

II. COMPUTATIONAL METHOD

Our system comprises of a Benzene wire cell, which is bonded between these electronic metallic's (gold), which are positioned [111] & [100]. Our model, we consider a Benzene wire molecule with multiple rings directed and held in the plane, the rings being kept in the plane by forcing planarity. For convenience, a system divided into two subspaces, electrodes & a central body (Fig- 1).

Revised Manuscript Received on March 30, 2020.

* Correspondence Author

Amardeep*, Amardeep, PhD, Electronics Engineering, IKGPTU Jalandhar, (Punjab) India. E-mail: amardeep22@gmail.com

Dr. Vijay Kumar Lamba, Professor, Global College of Engineering and Technology, Kahnpur Khui, (Punjab) India.

Email: lamba_vj@hotmail.com

© The Authors. Published by Blue Eyes Intelligence Engineering and Sciences Publication (BEIESP). This is an open access article under the CC BY-NC-ND license (<http://creativecommons.org/licenses/by-nc-nd/4.0/>)

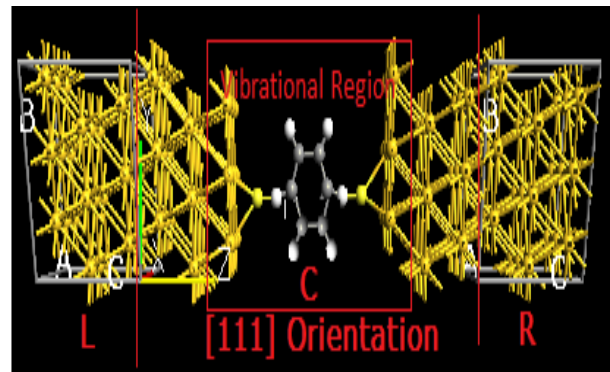


Figure-1. Benzene molecular wire (1 Rings), bridged between the two gold [111] probe, the angle of spinning about an axis by 60°, tilted by 30°

The centre body, called the extended molecule, comprises a wire molecule over 3- layers of the upper gold atom of 2- electrodes. We employ that provision to:

- incorporate effects of molecules and metals into fixed calculations,
- enter the "molecule" view to correct the decrease of the molecule,
- simplify the process and minimize computation time on implementing the idea of an expanded molecule.

We have applied an Ab-Initio Density Function Theory integrate with the Green Equivalent (NEGF) method for evaluating (i) regenerative geometries (ii) vibrational structures, (iii) vibration waves, (iv) integration of electric vibration modes (Integration of electron-phonon). To find geometries of the molecules bonded to the gold surfaces, geometric relaxation to be performed for the atomic coordinates and surface gold atoms, that is, the energy region shown in the (Fig. 1). The Boundary terms are used to calculate the unit cells containing one molecule plus one atom. -54 Au (6- layers of 3 X 3) to act for Au (111) surfaces. [13-16-16] Geometry optimization [17] is repeated as various lengths of a unit cell within a perpendicular direction to the surface to obtain (local) energy minimal. Winds are studied adopting small differences. The vibrational matrix (Hessian) of the total vibration region is obtained from a force exerted by removing all atoms in three directions by the factor of 0.02. The electron-phonon pairings ($M^{(\lambda)}$) are achieved from vibrational modes ($v^{(\lambda)}$) & derivative of Hamiltonian (H)¹

$$M_{ij}^{(\lambda)} = \sum_{\alpha} \sqrt{\frac{\hbar}{2m_{\alpha}\omega_{\lambda}}} \langle i | \frac{\partial H}{\partial R_{\alpha}} | j \rangle v_{\alpha}^{(\lambda)} \quad --1$$

here $\{|i\rangle\}$ is a basis set, m_{α} is mass of an atom corresponding to a nuclear coordinate R_{α} , and ω_{λ} is an angular frequency of mode λ . Based on the Hamiltonian calculate the method of total variance¹⁸. For limiting the scope of electron-phonon pairing, interactions are presumed to be neglected without the support of the device (Fig- 1);

e.g., the coupling considered to be bounded to molecule & the first 2- layers of the gold atoms on the surface.

It is currently intended to adopt the NEGF method in an (LOE) “lowest order expansion”. [18-20] This proximity is based on the two hypotheses: (i) the expansion to the lower order of electron accumulation and (ii) the infinite mass of the device & its contacts near Fermi energy. For the molecules we have studied here, the 1st proximity is rationalized because the electrons interrelate weakly with the sounds. It is very arduous to strongly force the 2nd approximation because the calculated transfer function stretch near around to the Fermi energy of molecules we studied here. The calculations, we have performed, cover the thermal effects of vibration modes. For finding the number of quanta of vibration in every mode, we set the condition such as the energy exchange rate between the electronic and the vibration modes is zero for all vibrations; e.g. the catalytic processes were measured by the formation of two pairs of electrons (electron density). To simplify the calculation, we use lower temperature limit & solve for quanta $n\lambda$ value for vibrational quit as a function of bias voltage (V)

$$n_\lambda = \frac{\gamma_{em}^{(\lambda)}}{\gamma_{eh}^{(\lambda)}} \times \begin{cases} 0; & |eV| < \hbar\omega_\lambda \\ |eV/\hbar\omega_\lambda| - 1; & |eV| \geq \hbar\omega_\lambda \end{cases} \quad --2$$

here $\gamma_{eh}^{(\lambda)} = \omega_\lambda Tr[M^{(\lambda)}A_1M^{(\lambda)}A_2]/\pi$ is electron-hole damping rate and the vibration emission constant $\gamma_{em}^{(\lambda)} = \omega_\lambda Tr[M^{(\lambda)}A_1M^{(\lambda)}A_2]/\pi$ is expressed in terms of electron-phonon coupling ($M^{(\lambda)}$), the spectral densities resulting from two contacts A_1 & A_2 , and the elastic spectral function ($A = A_1 + A_2$).

Electronic features of closed & bound quantum systems build on the DFT-NEGF applying numerical data sets. The lead parameter for consistency is the matrix density. In unbarred systems, the density matrix is calculated by applying NEGF. While in closed preference to temporal systems are calculated by using additions from Kohn-Sham Hamiltonian. Here Density Matrix describes the inequalities of electrons, & the density of electrons determines the effective energy recognized “Hartree exchange-correlation energy”. In the DFT, electronic formation of a system expressed in details of an electron Kohn-Sham Hamiltonian
$$H_{1el} = -\frac{\hbar}{2m} \nabla^2 + V^{eff}[n](r) \quad --3$$

Here, 1st term relates kinetic energy of an electron, while the 2nd term relates the electromagnetic force that travels in the field of energy from the other electrons, in which the other electrons are defined according to the mass of the electrons n . Here, the one-electron eigen-states are found by explaining one-electron Schrödinger equation

$$H_{1el}\psi_\alpha(r) = \varepsilon_\alpha\psi_\alpha(r) \quad --4$$

To solve this differential equation we enlarge the wave functions in a set of basic functions

$$\psi_\alpha(r) = \sum_i C_{\alpha i} \phi_i(r) \quad --5$$

This remodel the differential equation within a matrix equation for determining $C_{\alpha i}$

$$\sum_j H_{ij} C_{\alpha j} = \varepsilon_\alpha \sum_j S_{ij} C_{\alpha j} \quad --6$$

The Hamiltonian matrix, $H_{ij} = \langle \phi_i | H_{1el} | \phi_j \rangle$, and overlap matrix $S_{ij} = \langle \phi_i | \phi_j \rangle$, are given by 3D integrals above the basic functions. Thus an electron density of a system is given by

$$n(r) = \sum_\alpha |\psi_\alpha(r)|^2 f\left(\frac{\varepsilon_\alpha - \varepsilon_F}{kT}\right) \quad --7$$

Here $f(x) = 1/(1 + e^x)$ is Fermi function, ε_F is Fermi energy, and T is an electron temperature. Further the current is intended from the transmission coefficient using [18, 20]

$$I(V_L, V_R, T_L, T_R) = \frac{e}{h} \int T(E) \left[f\left(\frac{E - E_F^L + eV_R}{k_b T_R}\right) - f\left(\frac{E - E_F^L + eV_L}{k_b T_L}\right) \right] dE \quad --8$$

Here (f) is Fermi function, and T_L & T_R are electron temperatures for left & right electrodes. $T(E)$ is a transfer bond. In the calculations, the Perdew-Burke-Ernzerhof (PBE) gradient approximate (GGA) techniques are used. Hamiltonian overlap and the electronic densities are evaluated in a real-time grid defined with a cut-off wavelength of 150 Ry to attain a balance between precision calculation & accuracy. Larger electrons are directed through the Troulfer-Martins unseal pseudo, and the valence electrons are enlarged in the SIESTA local core set. The approach allows for absolute treatment of the electrode-molecule-electrode conjugation constant for a zero bias & partial bias & incorporates the outcome of the extraneous electric field caused by the selectors of the molecules.

III. RESULTS

The molecular wires, we simulated here have one, two, three, four, five and seven bond benzene rings shown in fig-2. After the geometry correction applying Gaussian-03 package, we adopt a SIESTA program combination to calculate the HOMO-LUMO metal gap of cells (fig. 3), to probe a two-probe system which means that the cell cables are positioned between the gold electrode (fig. 1) with potentials [111] and [100], to find the correct space among the gold molecules, and the space between the molecule molecules & the adjacent gold electrode of each cellular system.

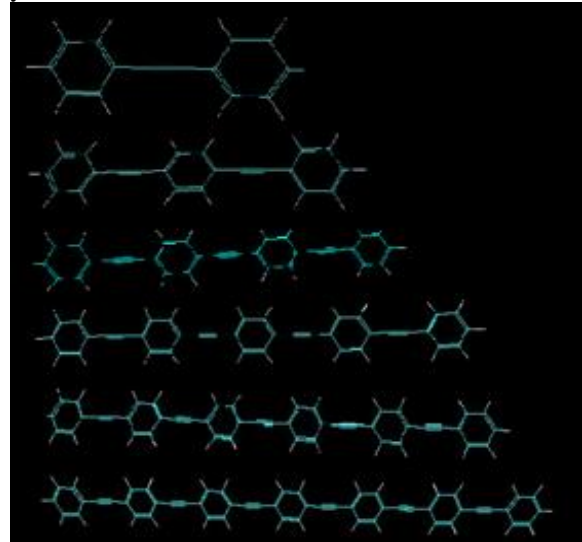


Figure-2. Different structures of benzene rings.

The coupling among molecule & the Au electrodes sports a vital role in electronic mobility because it moves & expands at a molecular level and alters the HOMO-LUMO gap differently due to their unique electronic properties. The coupling extends these levels of innumerable cells to the continuous observation of the density of surfaces. From figs. 3, one can notice that subsequently being bound with two Au stones, HOMO-LUMO gaps are completely enhanced by the interaction among molecule and electrodes.

The HOMO-LUMO gaps increase with the increase of no rings for both the solitary molecules and the sandwiched molecules. The variation within the HOMO-LUMO spaces by the length of the molecule will regulate the length of the behavior dependence. As for the length of the molecule increases, the HOMO-LUMO gap increases & the intersection of the HOMO and LUMO tails becomes larger.

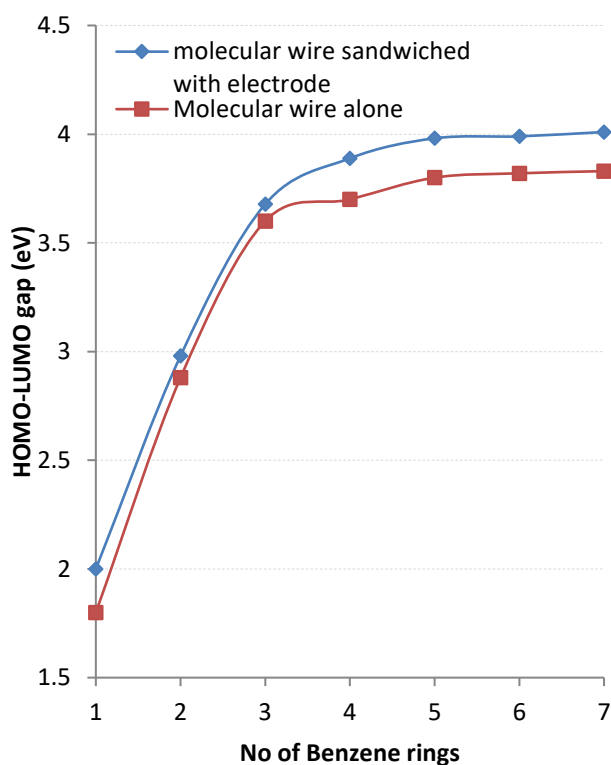


Figure-3. With the increase in several benzene rings within the molecular wire, the effective value of the HOMO-LUMO gap initially increases exponentially due to tunnelling & more linearly due to hopping.

Table 1
COUPLING PARAMETERS FOR BENZENE WIRE SANDWICHED BETWEEN A GOLD ELECTRODE

System	Distance	Coupling Parameter	System	Distance	Coupling Parameter
1 Ring	1.9	0.234	2 Ring	1.9	0.234
3 Ring	1.9	0.233	4 Ring	1.9	0.234
5 Ring	1.9	0.232	6 Ring	1.9	0.232
7 Ring	1.9	0.233	8 Ring	1.9	0.233

Which roots the transmission coefficient about E_F to be elevated arise in an increase of coupling constant shown in (table 1).

The conclusion will only be applicable when the electronic composition and distance of the molecule-electrode does not change notably while its fluctuations are still changed. Currently, the cell line is rotated around the bottom of the "atom" and then

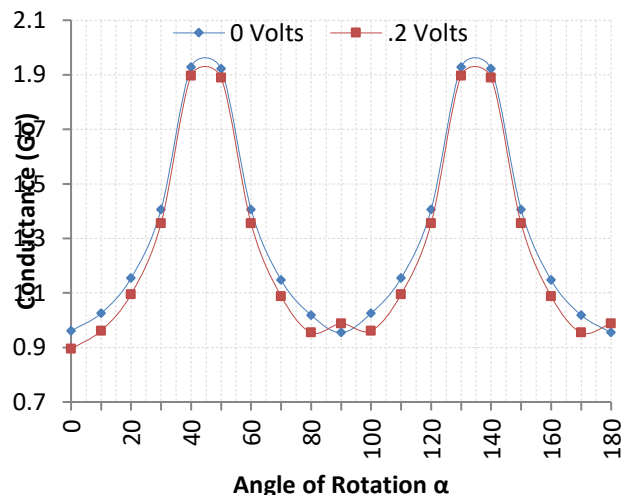


Figure-4. Change in conductance when a molecule wire with Benzene rings is revolved about the bottom "atom" from 0° to 180°

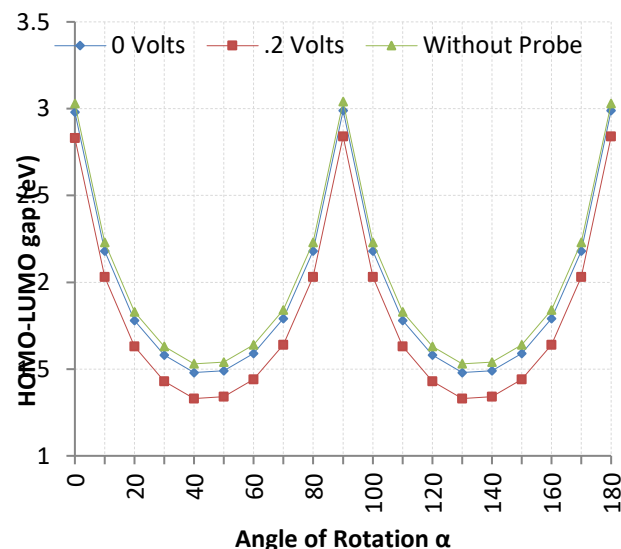


Figure-5. Change in HOMO-LUMO gap when a molecule is revolved about the bottom "atom" from 0° to 180°

shift the angle θ among the main axis of chain & the surface normal to it. As θ shifts, the p orbitals remain oriented horizontally to the molecular "backbone". The bond lengths of molecule-electrode do not change with θ , and the surfaces of two electrodes constantly remain parallel, and the distance among LUMO & HOMO is $E_{LUMO} - E_{HOMO} = 2t_\pi$ (were t_π is hopping among those π orbital's). The centre of the gap corresponds to the chemical energy of the examination at ($V = 0$) zero bias voltage. So from figs. 4 & 5 we conclude with benzene wire accompanied by planar structures (angles of 0° or 180°) having a much better

performance than a string with curved structures (inner angles close to 90°) because of smaller band spaces, the better orbital understanding of the electron.

From Figures 6 & 7 we find that when we press the benzene thread through the two rings initially the HOMO-LUMO gap increases and then decreases due to P and b orbital reductions. For example, where the habituation is the peak of the activation of the surface it is high and as the angle changes, it is due to the change of constant coupling between the electrode and the molecule or Bridge element.

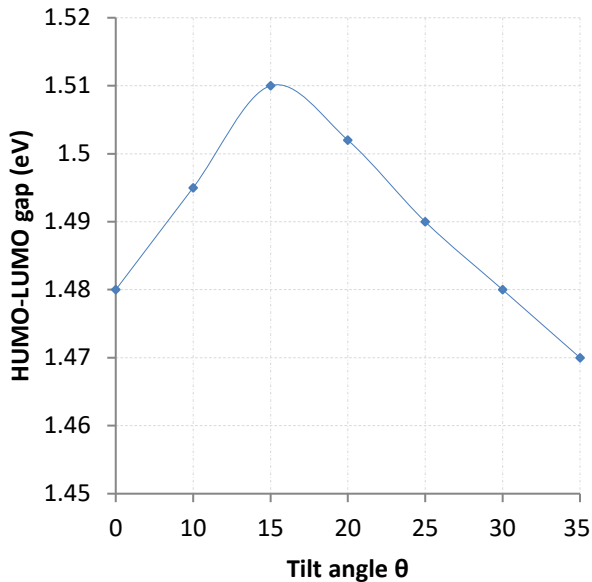


Figure-6. Change in the HOMO-LUMO gap while molecule wire along benzene rings is revolved around the bottom “atom” and thereby shift the angle θ among the main axis of the chain & the surface normal to it.

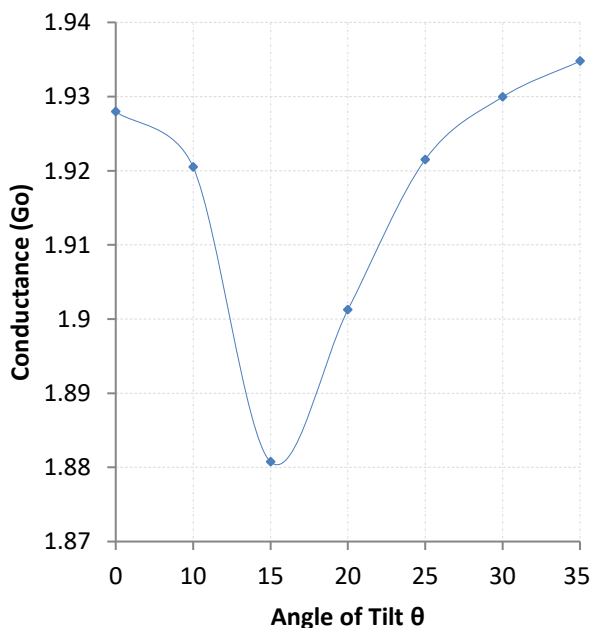


Figure-7. Change in conductance during a molecule wire with Benzene rings is revolved about the bottom "atom" & thereby shifting angle θ between the main axis of the chain & the surface normal to it.

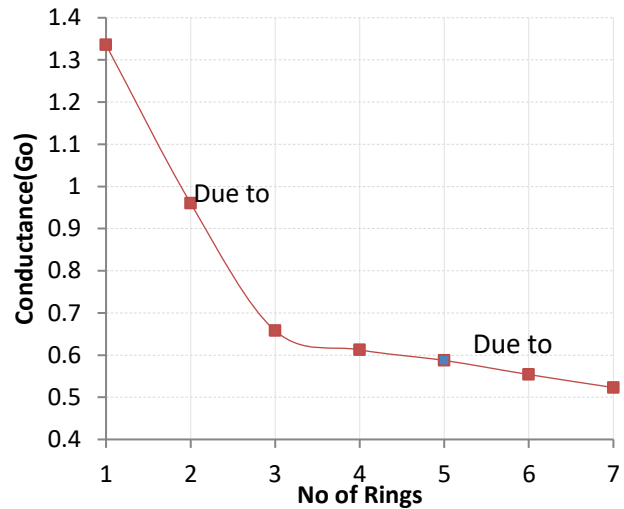


Figure-8. Change in conductance escorted by the increase in some benzene rings.

From graph, as shown in figure 8 we observe that conductance decline visually until the chain dimension is small which means that it contains four to five molecules of benzene but as we add on more molecule the change in conductance become linear, that can be explained that the conductance behaviour of system changes from tunnelling to hopping as the length of nanowire dimensions increases. Also, we observe that the performance of the system containing the number of benzene molecules is higher than their previous plan which means that the performance of the compounds 2, 4, 6, & 8 is greater than 1, 3, 5, & 7 respectively, which would indicate that the geometric equations of the molecules are the benzene-molecule and the unusual are inconsistent, leading to inconsistent contact interactions between the electrode and the wire, and the results show that the parameter for the binding of benzene molecules is greater than that of the benzene molecule chain. As we know, in the discriminatory argument for inequality is given by

$$R = R_0 \exp(\beta L) \quad \text{--9}$$

here R_0 is effective contact resistance, $\beta = 2(2m^*\phi)^{1/2}/\hbar$ is a structure-reliant tunnelling attenuation factor a particular rely on effective tunnelling barrier height (ϕ) and for our calculations it is 0.1 \AA^{-1} , the electron effective mass m^* , and Planck's constant, (L) is the molecular length. The tunnelling barrier height (ϕ) is usually approximated as energy distinction among the Fermi level, E_F & the closest frontier orbital, e.g., E_{HOMO} . For hopping, junction resistance follows,

$$R = R_0 + \alpha L = R_0 + \alpha_\infty L \exp\left(\frac{E_a}{kT}\right) \quad \text{--10}$$

here again, R_0 is a contact resistance, $\alpha = \alpha_\infty \exp\left(\frac{E_a}{kT}\right)$ is molecule specific parameter with units resistance per unit length, (L) is the molecular length, and (E_a) is the activation energy correlates with hopping.

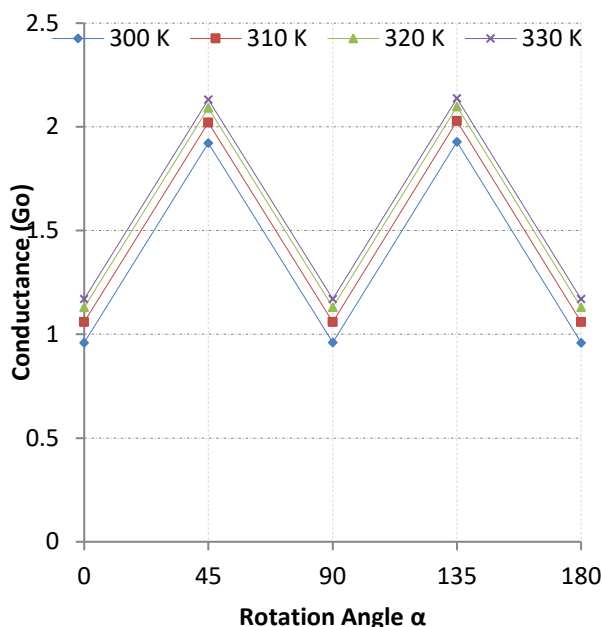


Figure-9. Change within conductance during a molecule is tilted at different temperatures.

So the tunnelling in general order has a much longer dependency than the jump. We, therefore, found so if we went to thermal stimulating of the cell membrane, there would be a modification within conductance as temperature increased, the movement of nuclei increased within the rings of cells containing cellular wires, and consequently the possibility of bond rotation & elasticity, leading to a tendency good geometry that promotes electronic integration and charge migration as shown in fig 9

IV. CONCLUSION

We conclude that:

- As the benzene rings are increased, the conductance decreases and the HUMO-LUMO gap increases exponentially.
- By tilting the benzene rings we could achieve the desired results witching points are attained at angle 45 degree.
- If we rotate the benzene ring axially, the conductance gets increased and the HUMO-LUMO gap gets decreased and
- Conductance increases with increases in temperature at different angles.

REFERENCES

1. H. Shirakawa, E. J. Lewis, A. G. McDiarmid, C. K. Chiang, and A. J. Heeger. J. Chem. Soc., Chem. Commun. 578–580 (1977).
2. A. Aviram and M.A. Ratner. Chem. Phys. Lett., 29-277, (1974).
3. N. Nitzan and M.A. Ratner. Science, 300(1384), (2003).
4. 2004 International technology roadmap for semiconductors. <http://public.itrs.net>.
5. J. Ulrich, D. Esrail, W. Pontius, L. Venkataraman, D. Millar (2005) and L. Doerr. J. Phys. Chem. B, 110(2462), (2006).
6. C. R. Kagan, A. Afzali, R. Martel, L.M. Gignac, P.M. Solomon, A.G. Schrott, and B. Ek. Nanoletters, 3(119), (2003).
7. A. Aviram and M. A. Ratner. Chem. Phys. Lett. 29, 277–283 (1974).
8. G. M. Whitesides and B. Grzybowski. Science 295, 2418–2421 (2002).
9. B. Franklin. Philos. Trans. R. Soc. London 64, 445–460 (1774).
10. A. Pockels. Nature 43, 437–439 (1891).
11. K. B. Blodgett. J. Am. Chem. Soc. 57, 1007–1022 (1935).
12. B. Mann and H. Kuhn. J. Appl. Phys. 42, 4398–4405 (1971).

13. E. E. Polymeropoulos. J. Appl. Phys. 48, 2404–2407 (1977).
14. R. G. Nuzzo and D. L. Allara. J. Am. Chem. Soc. 105, 4481–4483 (1983).
15. M. A. Reed, C. Zhou, C. J. Muller, T. P. Burgin, and J. M. Tour. Science 278, 252–254 (1997).
16. H. Haick, J. Ghabboun, and D. Cohen. Appl. Phys. Lett. 86, 042113 (2005).
17. T. W. Kim, G. Wang, and T. Lee. Nanotechnology 18, 315204 (2007).
18. Y.-L. Loo, D. V. Lang, J. A. Rogers, and J. W. P. Hsu. Nano Lett. 3, 913–917 (2003).
19. A. Vilan and D. Cohen. Adv. Funct. Mat. 12, 795–807 (2002).
20. K. T. Shimizu, J. D. Fabbri, J. J. Jelencic and N. A. Melosh. Adv. Mat. 18, 1499–1504 (2006).

AUTHORS PROFILE



Amardeep Amardeep is currently pursuing PhD in Electronics Engineering, at IKGPTU Jalandhar, (Punjab) India.
E-mail: amardeep22@gmail.com



Dr. Vijay Kumar Lamba Dr. Vijay Kumar Lamba is Professor at Global College of Engineering and Technology, Kahnpur Khui, (Punjab) India.
Email: lamba_vj@hotmail.com
Published about 50 papers in journals.